Diagnosis of Atrial Ectopic Origin from the Body Surface ECG: Insights from 3D Virtual Human Atria and Torso

Erick A Perez Alday[1], Michael A Colman[1], Tim D Butters[1], Jonathan Higham[1], Daniele Giacopelli[2], Philip Langley[2], Henggui Zhang[1]

[1]University of Manchester, Manchester, UK
[2]Newcastle University, Newcastle, UK

Abstract

Ectopic atrial activity underlies atrial tachycardia (AT), which, may predispose to atrial fibrillation (AF). Such abnormal excitation may be reflected as an alteration in the P-wave morphology (PWM) of the body surface potential (BSP).

Identifying the location of the ectopic foci from body surface potential maps, can help to diagnose the early onset of AF in a cost effective manner. However, the correlation between the PWM of BSP and the origin of atrial foci has not been well established.

In this study we use a biophysically detailed computational model of the human atria and torso to investigate such correlations.

1. Introduction

Atrial fibrillation (AF) is the most common sustained cardiac arrhythmia in the developed world [1]. It can predispose to heart attack, stroke and even lead to sudden death [2,3]. The current treatments of AF are relatively poor due to the incomplete understanding of the mechanisms underlying the genesis and maintenance of AF [4].

Recent studies have demonstrated that the pulmonary veins (PV) play an important role in initiating AF, and it is in this region the most numerous sites of ectopic foci and the dominant frequencies of atrial electrical excitation are observed [5,6].

Accurate and efficient diagnosis of AF is vital for designing strategies for AF treatment. Traditionally, the presence of AF can be non-invasively detected by the use of the 12 lead ECG, which shows characteristics of irregular saw-tooth P-waves in many of the 12-leads, with lead V1 often demonstrating a more regular saw-tooth morphology than the other leads [7]. However, the complex and rapid atrial electrical activity during AF makes it difficult to elicit further detailed information on the atrial activation using the 12 lead ECG alone.

Compared to conventional 12-lead ECG, multi-lead ECG systems may provide more information about the spatio-temporal dynamics of body surface potential (BSP) during atrial excitation. This may be useful for elucidating the origins of AF ectopic foci without the need of invasive methods, which may cause complications during surgery. However, the correlation between the characteristics of BSP distribution and atrial excitation patterns are unclear. The aim of this study was to use forward problem approaches of computational modelling of the heart and torso to explore possible correlations between atrial excitation patterns and BSP distribution.

2. Methods

Previously we have developed a detailed 3D model of the human atria and torso, which accounts for regional differences in atrial electrophysiology and is capable of producing regular sinus rhythm and irregular AF-like propagation patterns in the atria, reflected in the behavior of the BSP [8-10]. The primary limitation of this model however was in the simplistic and crude representation of the torso. For this study, we implement our most recent 3D human atrial model [10] and update the torso model, as describe below (section 2.2).

2.1. 3D Model of human atria

Briefly, the Colman *et al.* 2013 [10] model implemented a reaction diffusion equation to describe the propagation of electrical activity throughout the atria [11, 12]. The model equation was solved by the use of a finite difference method, at spatial and temporal resolution of $0.33 \times 0.33 \times 0.33$ mm3 and 0.01 ms, respectively. The anisotropy ratio, describing conduction longitudinal and transverse to the fibres is 10:1. In simulations, rapid point stimuli (mimicking atrial focal activity) were applied at different locations over the atria. Further details of the model parameters and protocol can be found in Colman *et al.* 2013 [10].

2.2. 3D torso model

The torso model was obtained from segmenting MRI images taken from the visible human dataset, for which the software ITK-SNAP [13] was used. The torso model mesh comprises of 14,224 surface elements and considers the presence of the lungs and liver (Figure 1 A), each of which have different electrical conductivity taken from Grimmes *et al* 2008 [14], and at spatial resolution of 0.33 × 0.33 × 0.33 mm^3. Within the 3D torso, the 3D model of the human atria was embedded to form the torso-atria model. For the 3D torso-atria model, the forward problem, describing propagation of electrical activity from the surface of the atria to the surface of the torso, was solved by the use of a boundary element method based in [15], and similar to [16]. Elements of the torso mesh corresponding to the locations of the placement of the electrodes in the 12 lead ECG were selected. Registered BSP signals from them were used to derive realistic P-waves (Figure 2 B).

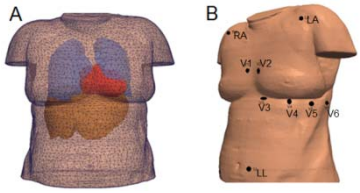

Figure 1. (A) The torso mesh of the model with the lungs (blue), heart (red) and liver (brown) in place. (B) Electrode positions for the 12-lead ECG on the torso mesh.

2.3. Ectopic focal beats

Ectopic focal activity was simulated, by applying a sequence of external supra-threshold electrical pulses with a cycle length of 700 ms at various locations of the atria. Each of the stimuli had amplitude of 2 nA and a duration of 2 ms, which applied to a spherical tissue region of radius 10mm. The BSP resulting from the third stimulus pulse were analysed.

3. Results

3.1. Validation of the simulated body surface ECG system

Simulated BSP maps during normal atrial excitation (*i.e.* sino-atrial node excitation) were compared to those observed experimentally (obtained from 64 lead ECG system) [17].

Qualitatively, the simulation BSP ECG data matched to experimental data in the activation time of the PWM as illustrated in Figure 2. In general, most of the BSP signals on the anterior part of the torso became positive (shown in red color) at the beginning of the activation. Then, the negative potentials (shown in blue color) appeared from the right superior (in both posterior and anterior part of the body) at around 40ms. The signals reached peak values at a time around 70ms. Therefore, a dynamic change in the direction of the dipole in the BSP was observed during the atrial activation.

Quantitative the simulated BSP ECG data also matched to experimental data. In simulations, the time interval between the P-wave peak and the first deflection of the P-wave was ~55ms, which was close to the experimental data of ~60ms.

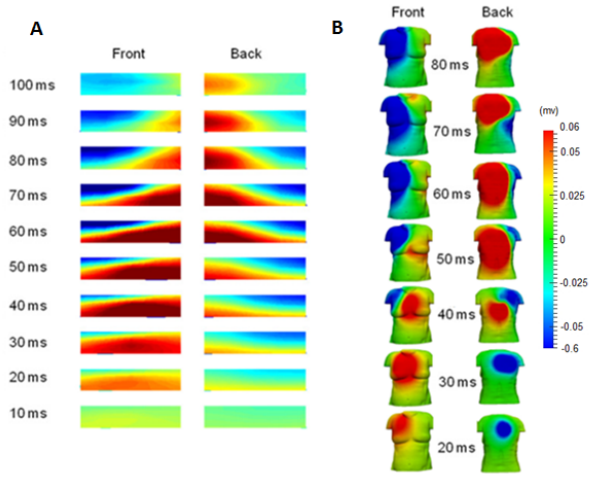

Figure 2. Comparison of the activation time between simulated BSP ECG P-waves and experimental data. (A) BSP obtained from 64-lead ECG P-waves from experiment [17]. (B) Simulation data. Amplitudes were normalized to the maximum from all 60 electrode positions in each subject.

3.2. Ectopic atrial activity and BSP correlation.

Our simulation results demonstrated marked differences in the spatio-temporal evolution of the BSP pattern resulting from different atrial activation sequences, associated with different locations of ectopic foci. This is illustrated in Figure 3, in which atrial activation sequences (Figure 3A) and snapshots of the BSP (Figure 3B) are shown for two different locations of ectopic foci; one was from the top of the right atrial appendage (Figure 3A(i)) and the other was the inferior vena cava (Figure 3A (ii)).

Briefly, atrial excitation originating from the right atrial appendage was reflected by an initially negative BSP in the right anterior and superior region of the torso, which then propagated towards the left posterior and inferior part of the body (Figure 3 B(i)).

When atrial focal activity originated from the inferior vena cava region, a negative signal (blue region) started from right inferior part of the body. In the posterior part

of the body, there was a larger region of negative polarity (blue part) as compared to the anterior part of the body (Figure 3B(ii)).

Results from both simulations clearly demonstrated a direct correlation between the activation pattern of the atria and the spatio-temporal distribution of the BSP. Such a correlation allowed us to develop an algorithm to identify the location of the atrial excitation origin from the BSP as described below.

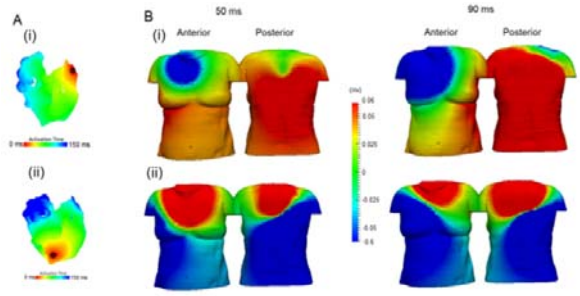

Figure 3. Correlation between body surface potential and atrial focal origins. (A) Atrial activation time in corresponding to atrial focal activity, originating from right atria appendage (i) and inferior vena cava (ii). Black dot marked the position of the atrial focal origins. (B) Snapshots of simulated BSP in the anterior and posterior torso surfaces at 50ms and 90ms.

3.3. Focus location algorithm

An algorithm based on analysis of the correlation between BSP dipole patterns and atrial focal origins was developed for identifying the location of atrial focal activity. The algorithm was based on signals of multi-lead ECG systems, with electrodes covering the majority of the anterior and posterior surfaces of the torso, but did not however require a specific number of leads, though the finer resolution of the BSP mapping the better of the accuracy of the algorithm.

In the algorithm, both of the torso and atria were divided into two sets of quadrants as shown in Figure 4. Of the torso, four quadrants in the anterior part of the body were labeled as Qt1 to Qt4; and four quadrants in the posterior part of the body were labeled as Qt5 to Qt8. Similarly, quadrants in the anterior part of the atria were labeled as Qa1 to Qa4, and the four quadrants in the posterior part of the atria were labeled as Qa5 to Qa8.

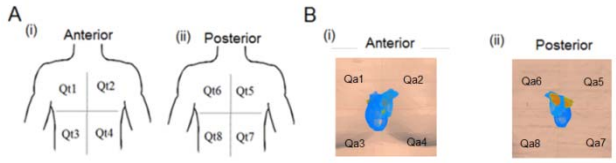

Figure 4. Schematic illustration of the quadrants in the torso and the atria. Qti indexes the quadrants of the torso (A), and the QAi indexes quadrants of the atria (B).

5 shows a schematic illustration of the algorithm that identifies the quadrant of the atria where the ectopic focus originates. As a negative P-wave (or BSP) at an electrode is associated with a wave travelling away from it, then the torso quadrant with negative P-wave is firstly determined, then the corresponding quadrant in the atria will be identified as the origin of atrial excitation. In implementation, each of the electrode sites was assigned a value dependent on the polarity of its P-wave: 1 for positive P-waves, 0 for biphasic and 2 for negative P-wave. Then, these values were summed for all the electrodes in each quadrant. The quadrant(s) with maximal value was determined.

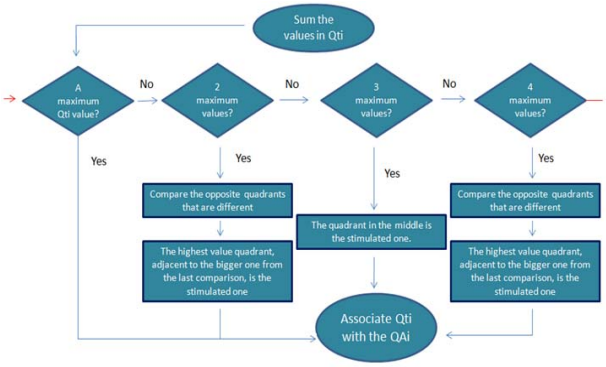

Figure 5. Schematic illustration of the algorithm to identify the quadrant of atrial focal origin based on 64-lead ECG P-wave values.

The algorithm was tested with 29 different cases. In 27 cases, the atrial focal location was correctly identified. Therefore, the success rate was 93%. The same data were tested by an extant Kistler's algorithm [18], which was based on 12-lead ECG. The success rate was 62% due to technique difficulty in classifying a bifid or biphasic P-wave as required by the algorithm.

4. Discussion

It is still difficult to investigate the correlation between origins of atrial excitation and BSP patterns in an experimental environment. In this sense, computational modelling provides a useful tool to investigate such a correlation, allowing us to develop an algorithm that can identify the atrial focal origin by using non-invasive multi-lead ECG systems.

In the present study, we have developed a computer model of 3D human atria-torso to simulate BSP patterns in corresponding to various atrial excitation patterns. The model was validated by comparing the simulated P-waves of different ECG leads and BSP dipole direction during normal sinus rhythm to experimental data. In simulations, it was shown that there was a strong correlation between PWM of the BSP and locations of ectopic atrial activity. Based on such correlation, a novel algorithm has been developed to identify atrial focal

origin from PWM of the BSP, which had a higher success rate as compared to the Kistler's algorithm [18] based on 12-lead ECG.

Similar to other computer models of cardiac tissues, the present 3D torso-atria model also has some limitations. One limitation is that the torso model lacks considerations of some other types of tissue and organs with different electrical conductivity, which may have impacts on the distribution of BSP. This limitation may affect the amplitude, but may not affect the direction of the BSP dipole, which is the focus of this study.

Another limitation of the model is the coarse spatial resolution of the defined quadrants in both of the torso and the atria. Due to this limitation, the identified atrial focal origin may fall in a quadrant that covers a significantly large portion of atrial tissue.

Nevertheless, this limitation can be improved by finer definition of the quadrants. In addition the model requires further improvements on modeling of PV regions, for which a more complete torso model would be useful.

Finally, validating the algorithm against experimental clinical data warrants future studies.

5. Conclusion

Our simulation data suggested that atrial ectopic activity can be reflected directly on changes of PWM of the BSP. This study established a correlation between BSP maps and ectopic activity presence, which requires detailed analysis of PWM registered from specific anterior-posterior leads.

Acknowledgements

This work was supported by CONACyT and EPSRC.

References

[1] Nattel S, Shiroshita-Takeshita A, Brundel BJJM, Rivard L. Mechanisms of atrial fibrillation: lessons from animal models. Prog Cardiovasc Dis 2005;48(1):9–28.

[2] Benjamin EJ, Wolf PA, D'Agostino RB, Silbershatz H, Kannel WB, Levy D. Impact of atrial fibrillation on the risk of death: the Framingham Heart Study. Circulation 1998;98(10):946–52.

[3] Anter E, Jessup M, Callans DJ. Atrial fibrillation and heart failure: treatment considerations for a dual epidemic. Circulation 2009;119(18):2516–25.

[4] Ehrlich JR, Nattel S. Novel approaches for pharmacological management of atrial fibrillation. Drugs 2009;69(7):757–74.

[5] Arora R, Verheule S, Scott L, Navarrete A, Katari V, Wilson E, et al. Arrhythmogenic substrate of the pulmonary veins assessed by high-resolution optical mapping. Circulation 2003;107(13):1816–21.

[6] Kumagai K, Ogawa M, Noguchi H, Yasuda T, Nakashima H, Saku K. Electrophysiologic properties of pulmonary veins assessed using a multielectrode basket catheter. J Am Coll Cardiol 2004;43(12):2281–9

[7] Fuster V, Rydén LE, Cannom DS, Crijns HJ, Curtis AB, Ellenbogen KA, et al. Guidelines for the management of patients with atrial fibrillation. Executive summary. Rev Esp Cardiol 2006;59(12):1329.

[8] Aslanidi OV, Colman MA, Stott J, Dobrzynski H, Boyett MR, Holden AV, et al. 3D virtual human atria: a computational platform for studying clinical atrial fibrillation. Prog Biophys Mol Biol 2011;107(1):156–68.

[9] Colman MA, Aslanidi OV, Stott J, Holden AV and Zhang H. Correlation between P-wave morphology and origin of atrial focal tachycardia-insights from realistic models of the human atria and torso. IEEE Trans Biomed Eng 2011;58(10):2952-2955.

[10] Colman MA, Aslanidi OV, Kharche S, Boyett MR, Garratt C, Hancox JC, Zhang H. Pro-arrhythmogenic effects of atrial fibrillation-induced electrical remodelling: insights from the three-dimensional virtual human atria. Journal Physiology, 2013.

[11] Rudy Y. From genome to physiome: integrative models of cardiac excitation. Ann Biomed Eng 2000;28(8):945–50.

[12] Clayton RH, Bernus O, Cherry EM, Dierckx H, Fenton FH, Mirabella L, et al. Models of cardiac tissue electrophysiology: progress, challenges and open questions. Prog Biophys Mol Biol 2011;104(1-3):22–48.

[13] Yushkevich PA, Piven J, Hazlett HC, Smith RG, Ho S, Gee JC, and Gerig G. User-guided 3D active contour segmentation of anatomical structures: Significantly improved efficiency and reliability. *Neuroimage* 2006;31(3):1116-28. www.itksnap.org.

[14] Grimmes S, Martinsen OG. Bioimpedance and Biolectricity Basics. 2nd edition, 2008.

[15] Salu Y. Implementing a consistency criterion in numerical solution of the bioelectric forward problem. IEEE Trans Biomed Eng 1980;27(6):338-341.

[16] Stott J, Kharche S, Law P, Zhang H. Simulating the effects of atrial _brillation in electrically heterogeneous human atria: A computer modelling study. Computers in Cardiology 2008:65-68.

[17] Giacopelli D, Bourke JP, Murray A, Langley P. Spatial pattern of P waves in paroxysmal atrial fibrillation patients in sinus rhythm and controls. PACE 2012; 35: 819-26.

[18] Kistler PM, Roberts-Thomson KC, Haqqani HM, Fynn SP, Singarayar S, Vohra JK, et al. P-wave morphology in focal atrial tachycardia: development of an algorithm to predict the anatomic site of origin. J Am Coll Cardiol 2006;48(5):1010–7.

Address for correspondence.

Erick Andres Perez Alday
Office 3.17, Schuster Building, Brunswick Street, M13 9PL, Manchester, United Kingdom
erickandres.perezalday@postgrad.manchester.ac.uk